Supporting Information

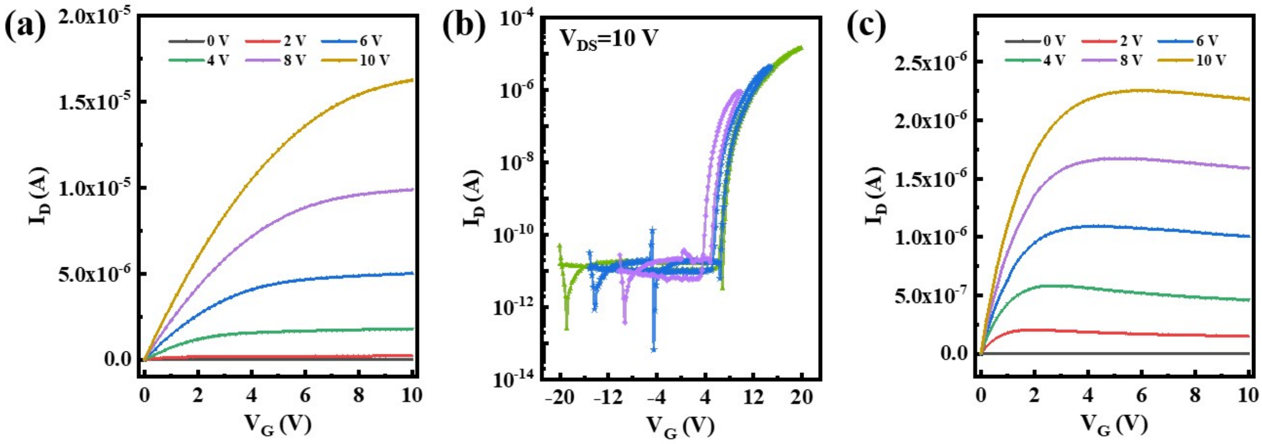

Figure. S1 (a) Output characteristics of the devices with a top PVA flat layer prepared with 4.0 wt% PVA dispersion liquid. (b) Transfer characteristics of the devices with Al_2O_3: Nd as the insulator layer. (c) Output characteristics of the devices with a top PVA layer prepared with 3.0 wt% PVA dispersion liquid.

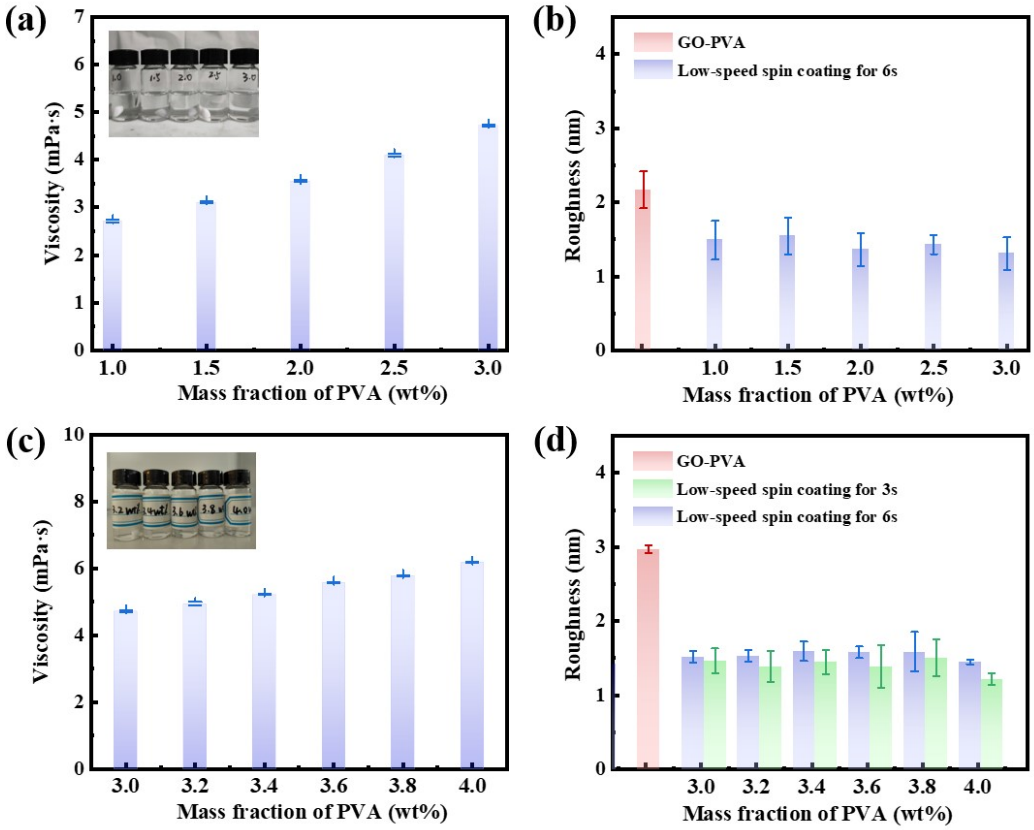

Figure. S2 (a) Viscosity of PVA dispersion liquids with different mass fractions (1.0-3.0 wt%). The inset shows the optical image of the dispersion liquids. (b) The roughness of GO-PVA/PVA stacked films with different top PVA layers (1.0-3.0 wt%). (c) Viscosity of PVA dispersion liquids with different mass fractions (3.0-4.0 wt%). The inset shows the optical image of the dispersion liquids. (d) The roughness of GO-PVA/PVA stacked films with different top PVA layers (3.0-4.0 wt%).

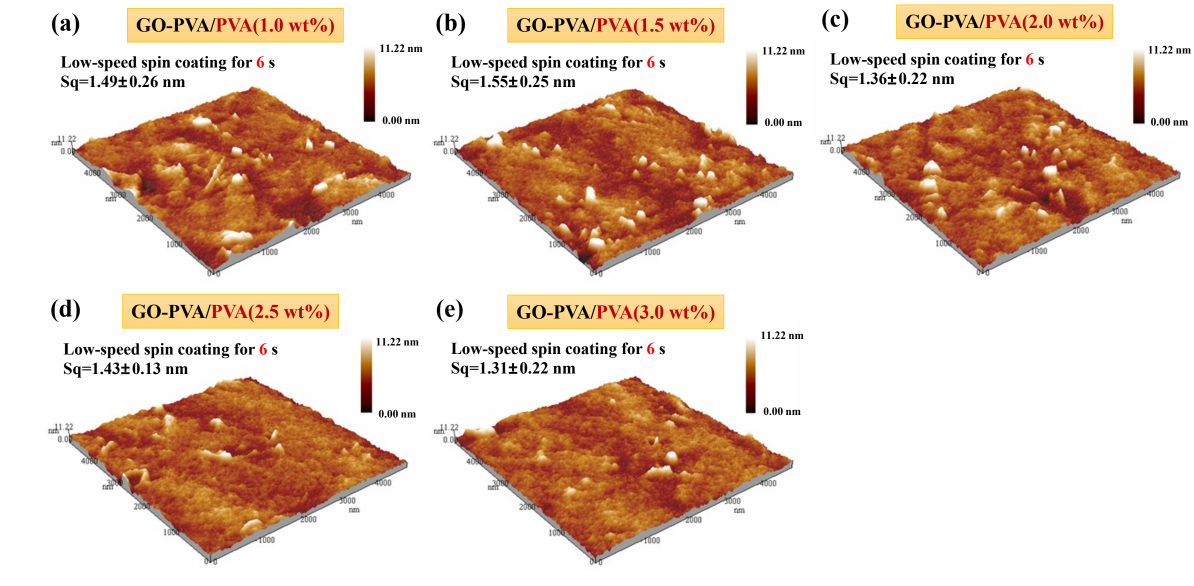

Figure S3. Surface morphology of GO-PVA/PVA films prepared from dispersion liquids with PVA mass fractions of (a) 1.0 wt%, (b) 1.5 wt%, (c) 2.0 wt%, (d) 2.5 wt% and (e) 3.0 wt%.

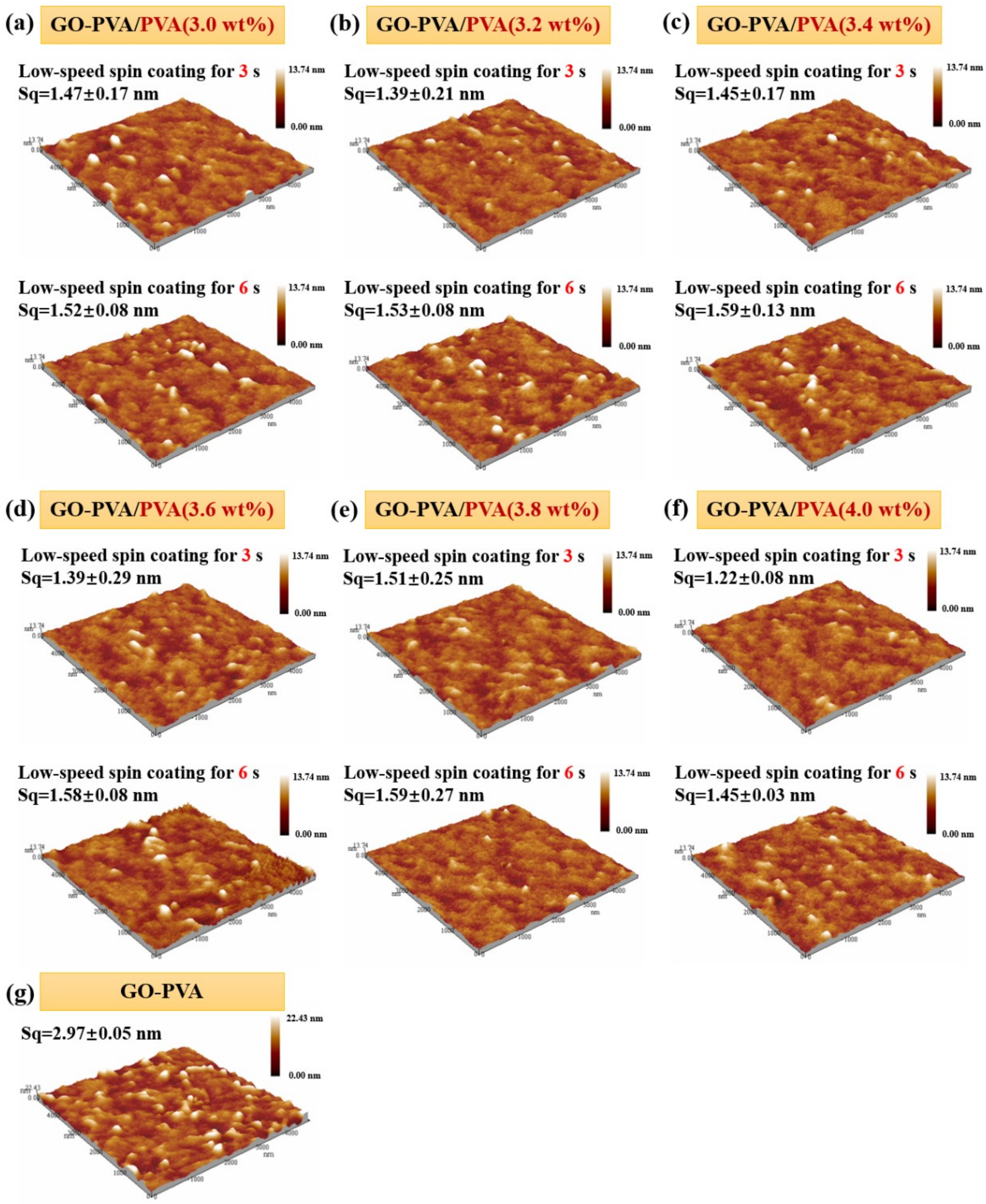

Figure S4. Surface morphology of GO-PVA/PVA films prepared from dispersion liquids with PVA mass fractions of (a) 3.0 wt%, (b) 3.2 wt%, (c) 3.4 wt%, (d) 3.6 wt%, (e) 3.8 wt% and (f) 4.0 wt% at different low-speed spin-coating times (3 and 6 s). (g) Surface morphology of GO-PVA films.

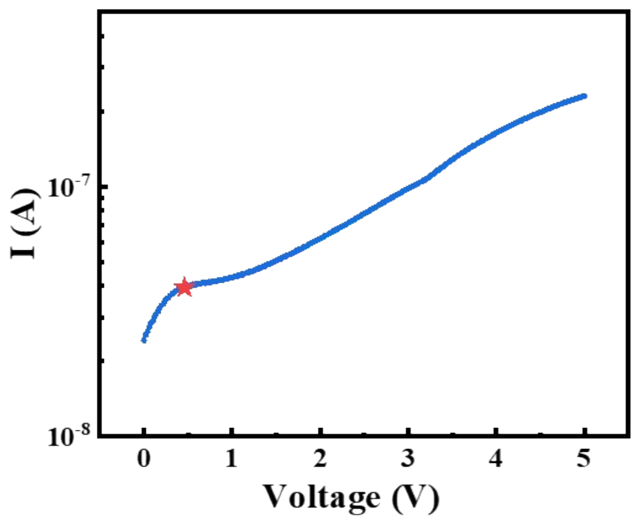

Figure S5. Leakage current of GO-PVA/PVA films.

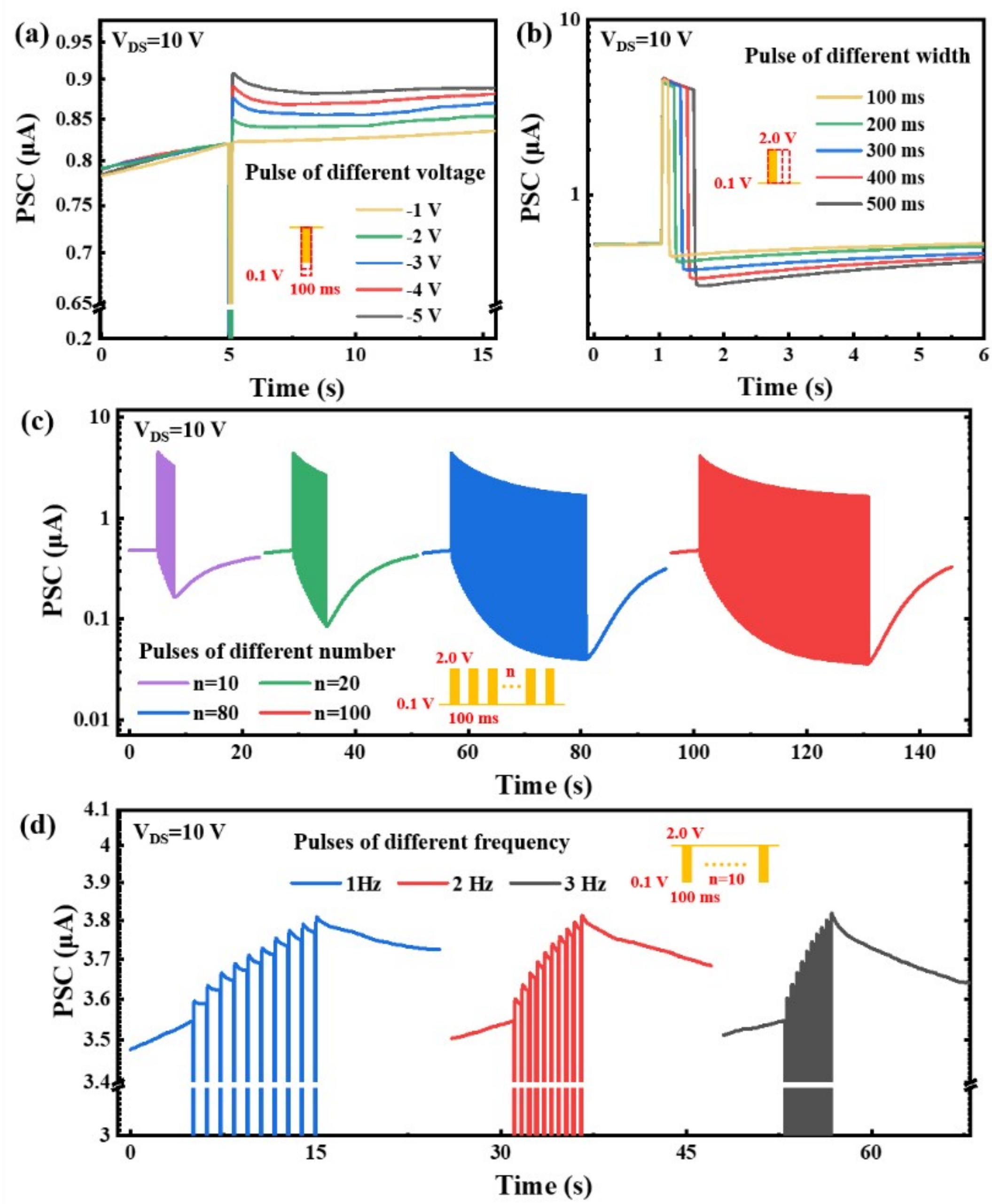

Figure S6. Characteristics of devices on a glass substrate: (a) EPSC triggered and modulated by input pulses with different voltages; (b) IPSC triggered and modulated by input pulses with different widths; (c) IPSC triggered and modulated by input pulses with different numbers; (d) EPSC triggered and modulated by input pulses with different frequencies.

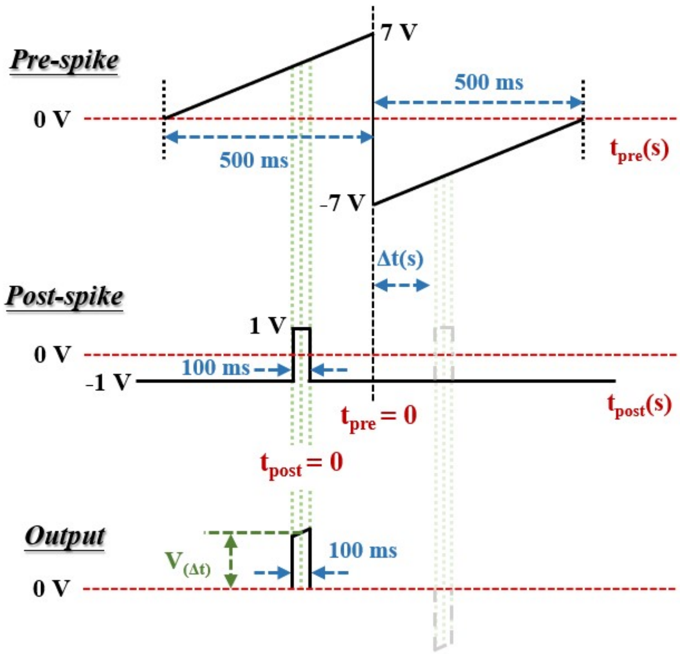

Input (V_{pre})	Control (V_{post})	Output (V_G)
0	1 V	0
	-1 V	
$V_{pre} \neq 0$	1 V	V_{pre}
	-1 V	0

Figure S7. Waveforms of V_{pre} (pre-neuron pulse), V_{post} (post-neuron pulse) and output V_G. The table is the logic of the multiplexer.

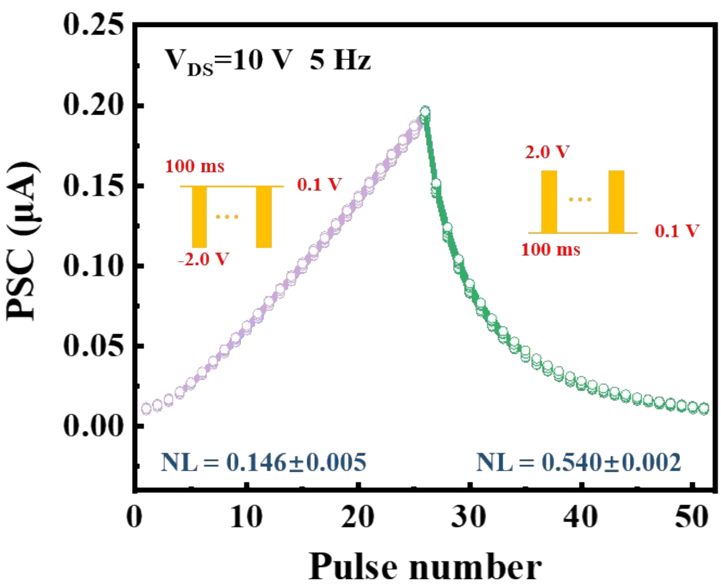

Figure S8. PD characteristics indicate that the update of synaptic weights is reproducible and stable. Each cycle consists of 25 identical voltage pulses (-2.0 V/2.0 V for 100 ms spaced 100 ms apart).

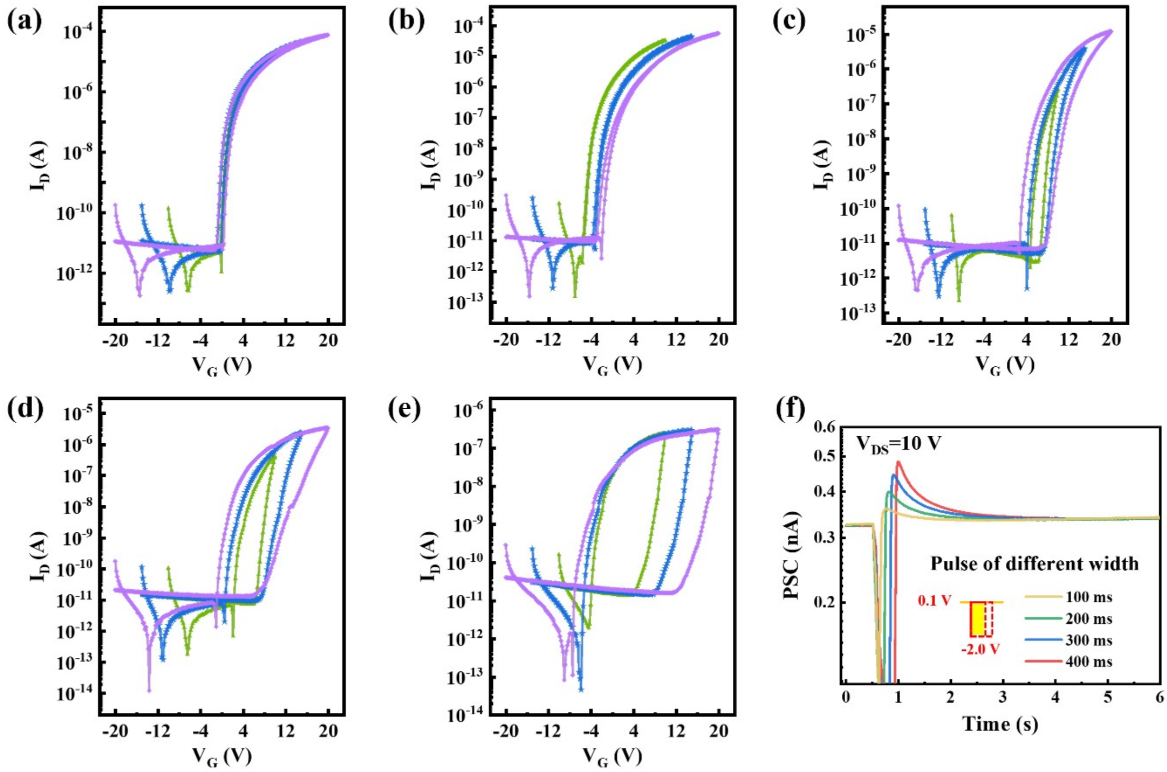

Figure S9. Transfer characteristics of GO-PVA single layer charge-trapping synaptic transistors with GO concentrations of (a) 0 mg/mL, (b) 0.2 mg/mL, (c) 0.4 mg/mL, (d) 0.6 mg/mL, and (e) 0.8 mg/mL over different V_G scan ranges; (f) EPSC of 0.8 mg/mL GO synaptic transistors triggered and modulated by pulsed signals (100-400 ms width).

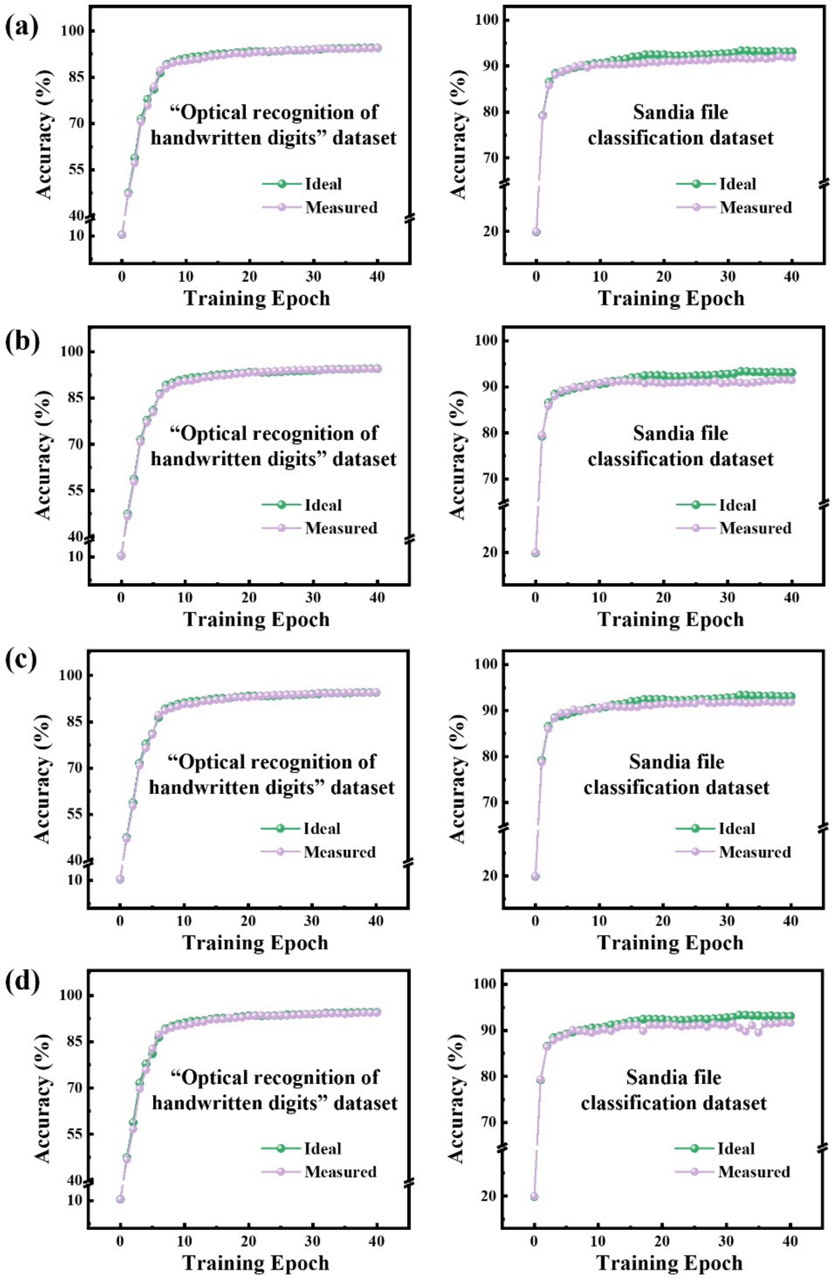

Figure S10. Recognition accuracy of (a) $T_{S\text{-}O}$ device, (b) $T_{D\text{-}O}$ device, (c) $T_{D\text{-}I}$ device, and (d) $T_{S\text{-}I}$ device on the "Optical Handwriting Digit Recognition" dataset and the Sandia file classification dataset versus the training epochs.

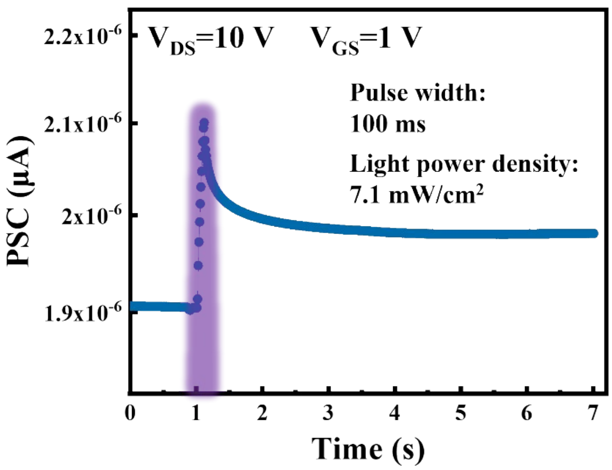

Figure S11. Response characteristics of the $T_{S\text{-}I}$ devices to ultraviolet light (365 nm) pulse.

Table S1. Electrical characteristics of thin film transistors (TFTs) with different insulator layer

Insulator layer	V_G (V)	I_{on}/I_{off}	ss (V/decade)	ΔV_{TH} (V)
Al_2O_3	-10~10	$(4.01 \pm 2.32) \times 10^5$	0.36±0.01	-1.3±0.1
	-15~15	$(4.03 \pm 0.46) \times 10^5$	0.22±0.04	-1.3±0.2
	-20~20	$(4.63 \pm 0.61) \times 10^6$	0.21±0.06	-0.1±0.2
Al_2O_3/ *(0.6 mg/mL)* GO-PVA/ *(4.0 wt%)* PVA	-10~10	$(2.36 \pm 0.11) \times 10^5$	0.35±0.01	-2.2±0.2
	-15~15	$(5.50 \pm 0.05) \times 10^5$	0.33±0.03	-0.2±0.1
	-20~20	$(8.85 \pm 0.18) \times 10^5$	0.36±0.02	2.09±0.4
Al_2O_3/ (0.6 mg/mL) GO-PVA/ *(3.0 wt%)* PVA	-10~10	$(1.58 \pm 0.66) \times 10^5$	0.37±0.02	5.2±0.2
	-15~15	$(2.99 \pm 0.14) \times 10^5$	0.35±0.00	8.3±0.3
	-20~20	$(6.09 \pm 0.16) \times 10^5$	0.35±0.02	10.2±0.4
Al_2O_3/ *(1.0 mg/mL)* GO-PVA/ *(3.0 wt%)* PVA	-10~10	$(1.18 \pm 0.48) \times 10^6$	0.16±0.01	11.1±0.2
	-15~15	$(1.89 \pm 0.64) \times 10^6$	0.19±0.00	16.7±0.1
	-20~20	$(2.15 \pm 0.60) \times 10^6$	0.21±0.01	24.8±0.2

Table S2. Electrical characteristics of synaptic transistors under different bending states

Device	V_G (V)	I_{on}/I_{off}	ss (V/decade)	ΔV_{TH} (V)
$T_{S\text{-}O}$	-10~10	$(3.80\pm3.54)\times10^7$	0.14±0.02	8.8±0.1
	-15~15	$(3.16\pm1.10)\times10^7$	0.09±0.04	15.3±0.1
	-20~20	$(8.69\pm5.91)\times10^7$	0.16±0.01	22.3±0.2
$T_{D\text{-}O}$	-10~10	$(1.23\pm0.18)\times10^6$	0.19±0.01	8.7±0.1
	-15~15	$(2.52\pm0.41)\times10^6$	0.22±0.00	16.1±0.1
	-20~20	$(2.92\pm0.40)\times10^6$	0.23±0.01	24.5±0.2
$T_{D\text{-}I}$	-10~10	$(7.31\pm0.58)\times10^5$	0.24±0.01	11.3±0.1
	-15~15	$(1.39\pm0.24)\times10^6$	0.24±0.00	19.2±0.2
	-20~20	$(2.42\pm0.60)\times10^6$	0.25±0.02	25.1±0.5
$T_{S\text{-}I}$	-10~10	$(9.83\pm3.97)\times10^5$	0.19±0.01	10.2±0.1
	-15~15	$(2.61\pm1.15)\times10^7$	0.18±0.03	17.4±0.1
	-20~20	$(4.03\pm3.26)\times10^7$	0.17±0.01	25.1±0.1

Table S3. PD characteristics and recognition accuracy of devices under different bending states

	Unbent devices	T_{S-O}	T_{D-O}	T_{D-I}	T_{S-I}
G_{MAX}/G_{MIN}	17.67±0.99	4.98±0.43	2.06±0.12	2.06±1.02	3.20±0.08
NL_P	0.146±0.005	0.173±0.011	0.055±0.001	0.033±0.003	0.053±0.003
NL_D	0.540±0.002	0.223±0.079	0.010±0.001	0.082±0.003	0.184±0.003
MNIST	93.7%	97.1%	94.7%	97.1%	95.6%
Optical recognition of handwritten digits	94.3%	94.5%	94.5%	94.4%	94.3%
Sandia file classification	91.4%	91.9%	91.4%	91.9%	91.7%